

Joint Visual-Temporal Embedding for Unsupervised Learning of Actions in Untrimmed Sequences

Rosaura G. VidalMata
University of Notre Dame
Notre Dame, IN
rvidalma@nd.edu

Walter J. Scheirer
University of Notre Dame
Notre Dame, IN
walter.scheirer@nd.edu

Hilde Kuehne
MIT-IBM Watson Lab
Cambridge, MA
kuehne@ibm.com

Abstract

Understanding the structure of complex activities in videos is one of the many challenges faced by action recognition methods. To overcome this challenge, not only do methods need a solid knowledge of the visual structure of underlying features but also a good interpretation of how they could change over time. Consequently, action segmentation tasks must take into account not only the visual cues from individual frames, but their characteristics as a temporal sequence of features.

This work presents our findings on the impact of incorporating both visual and temporal learning on an unsupervised action segmentation pipeline. We introduce a novel approach to extract relevant visual and temporal features from untrimmed sequences for the temporal localization of sub-activities within complex actions without any labeling information. Through extensive experimentation on two benchmark datasets – *Breakfast Actions*, and *YouTube Instructions* – we show that the proposed approach is able to provide a meaningful visual and temporal embedding from the visual cues from contiguous video frames and that it indeed helps in temporal segmentation.

1. Introduction

Research shows that humans usually understand complex activities through ongoing temporal segmentation of perceived input into meaningful segments [31]. Nevertheless, replicating this behaviour in fully automated systems is a challenging problem as it requires identifying the meaningful steps in a given task and how do they logically relate to each other. Fully supervised systems have been proposed to realize such a temporal segmentation, but they rely on large amounts of training data. However, annotating such data is especially expensive for temporal video segmentation as this task usually requires a dense frame-based annotation. Weakly supervised approaches attempt to allevi-

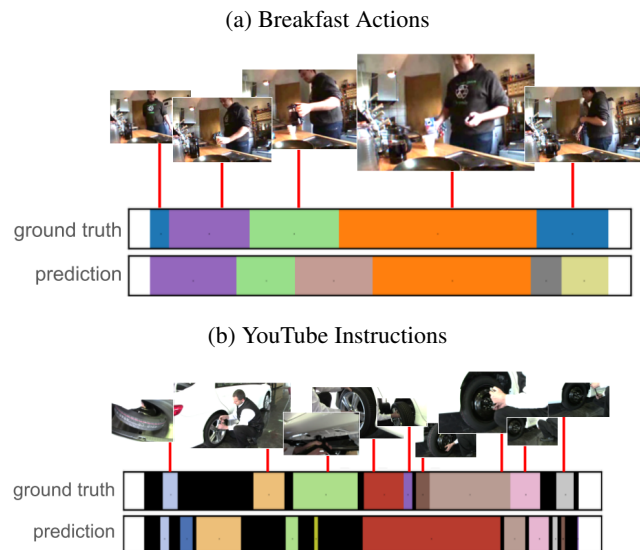


Figure 1: Temporal segmentation of two videos from the Breakfast Actions [12] and YouTube Instructional[2] Datasets. The black segments in the YouTube Instructions video signal background frames whose content is not associated to a sub-activity relevant to the video task. Our approach maintains the logical ordering of sub-activities and a good estimate on their start and duration.

ate this by incorporating the use of additional sources of information such as speech or video captions [2, 20], but most available real-world video data —such as surveillance data— does not come with any additional modality such as audio, subtitles, or descriptive meta-data. This makes it difficult for such approaches to translate to real-world applications.

Therefore, other methods have been proposed to address the problem of training such models without dense human generated labels, spanning from learning with weak or sparse annotation [9, 14, 16] to completely unsupervised learning of temporal action segmentation [4, 28, 15, 1]. The

here proposed work deals with the later problem, the unsupervised learning of action segments from unlabeled video data, which can be framed as the task of unsupervised temporal action segmentation. This follows the idea that, given a set of videos all capturing the same activity, it should be possible to identify temporal segments with similar sub-actions across all videos.

While the number of sub-actions in videos belonging to the same type of task is usually not constant, the order and temporal location in which certain activities occur is more stable. As such, in videos showing how to make pancakes the process of cracking eggs would not only look visually similar across all videos, but would generally occur before other tasks such as mixing the eggs into the batter or pouring the batter onto the griddle. So, sub-activities of a given task tend to not only share certain visual features, but also occur in a similar temporal space. Given this, recent approaches in the field usually focus on learning a strong temporal regularization [28, 15], but we argue that this might lead to a lower ability to identify segments based on their visual representation.

The proposed approach aims at addressing this problem and proposes a joint visual-temporal learning pipeline which combines the advantages of current temporal embedding systems with a visual embedding based on a combination of predictive visual and temporal learning tasks. To this end, we combine the recent best performing temporal embedding system [28] (multi-layer perceptron architecture designed to estimate the relative timestamp of a given video frame) with a visual encoder-decoder pipeline that is trained on a combination of visual loss and temporal loss.

The idea of this combination is that the decoding should not only reconstruct the plain input signal, but should also find a reconstruction that allows for a better estimation of the respective timestamp and, thus, a better temporal reconstruction. To prevent an overfitting of the proposed system, we shift the output of the visual encoder by one frame, which turns it into a visual prediction architecture, similar to other self-supervised models [21, 6]. Combined with the temporal loss, the encoder-decoder predicts a frame-representation that is optimized to give the best timestamp prediction in the temporal embedding framework. The resulting embedding space thus captures visual and temporal representations of each individual frame.

During training we further make use of a freeze-unfreeze protocol, training the visual embedding first, then freezing those layers and refining the temporal embedding separately. It shows that this protocol is especially helpful for sequential videos with only weak visual cues where a combined training is not feasible. We evaluate the proposed system on two challenging standard benchmark datasets, the YouTube Instructions dataset [4] and the Breakfast dataset [12] with respect to various metrics. Figure 1 shows quali-

tative examples which demonstrate that the proposed architecture is able to adapt well to a diverse set of action tasks and achieve good quality temporal segmentations up to par with current state-of-the-art approaches.

We summarize our contributions as follows:

- A state-of-the-art approach for the unsupervised temporal segmentation of actions in video incorporating visual and temporal features in a self-supervised manner.
- An extensive evaluation on the influence of temporal learning tasks on sub-action clustering and segmentation.

2. Related Work

2.1. Unsupervised learning of temporal sequences

While there has been plenty of work done in the area of action segmentation in video, a vast majority of the approaches rely on frame annotations –fully supervised methods– [9, 7, 13, 25], or some form of metadata –weakly supervised approaches– [16, 5, 24]. Such models achieve high quality temporal segmentations but their training is heavily dependent on vast amounts of good quality training labels which can be prohibitive in most real life scenarios. Despite these limitations, there has been few research conducted in unsupervised methods to help overcome the dependence on labeled data.

One of the first methods to address this issue is the one proposed by Bojanovski *et al.* [4] based on a Frank-Wolfe optimization algorithm. Sener *et al.* [28] later proposed the modelling of the temporal structure of sub-activities using a combination of Generalized Mallows Model (GMM) sampling and the estimation of the action length (calculated using the frame distribution) to estimate sub-activity segmentation in complex action videos. Following a similar segmentation pipeline, Kukleva *et al.* [15] propose instead a combination of temporal encoding (generated using a frame timestamp prediction network) and a Viterbi decoding for consistent frame-to-cluster assignment. On the other hand, Aakar *et al.* [1] approach the unsupervised segmentation task with a predictive learning framework which uses the difference between observed and predicted frame features as a means to determine event boundaries, as such working on a per video-based segmentation.

2.2. Unsupervised and self-supervised learning of visual representations

Complementary, a lot of different methods have been proposed for the learning of visual representations without labels [11]. Particularly, in the case of learning video representations in an unsupervised way, various approaches

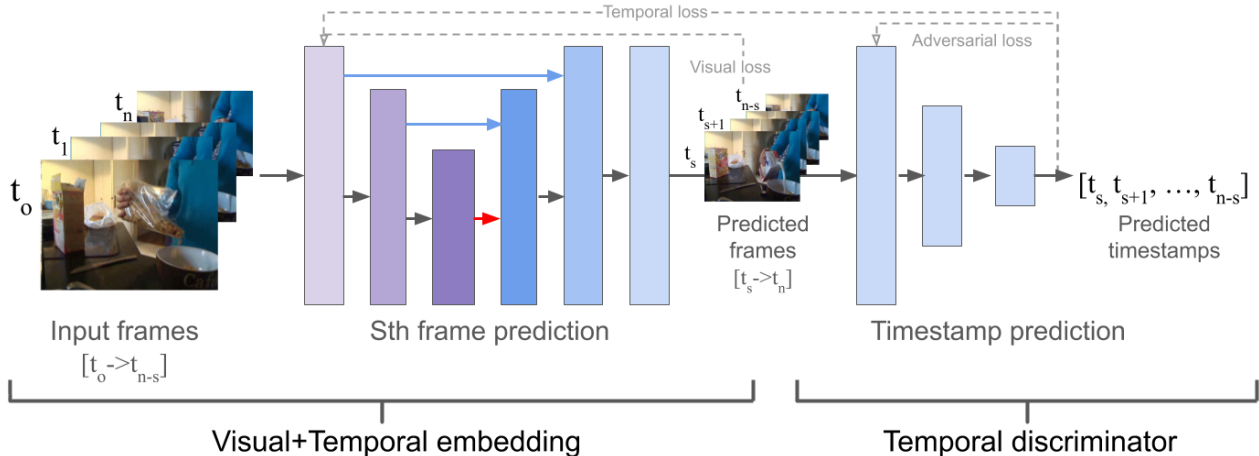


Figure 2: Two stage visual-embedding pipeline: 1) Visual+Temporal embedding: next frame prediction U-Net to generate a visual-temporal embedding (output of the last down-sampling layer, denoted by a red arrow), 2) Temporal discriminator: timestamp predictor MLP used to identify the loss of temporal information in the frames predicted by stage 1.

make use of temporal properties of the data *e.g.* in form of shuffling [23], or similar to the here proposed idea, temporal prediction [29, 6].

Temporal prediction has been established as a way to achieve a deeper understanding of the data ([29, 19, 30]) as it requires an implicit understanding of the structure of the observed visual features and the rules they follow while they change over time. However, it has been pointed out that the use of traditional losses does not translate well for video frame prediction. Srivastava *et al.* [29] have observed that predictive models trained solely with an MSE loss have a tendency of blurring regions with uncertainty. This has given way to the introduction of promising alternatives such as the adversarial loss present in Generative Adversarial Networks (GANs) [8] and Conditional GANs [22] which has led to significant advances in the performance of video prediction [6, 18, 21]. Similar to our approach, GAN-based methods have incorporated the use of U-Net architectures [27] into their generator module given their good performance in image-to-image translation [10, 32] and image segmentation [27, 3, 17] tasks.

3. System description

Given a collection $D_A = \{v_i\}_{i=1}^V$ of V complex activity videos belonging to the same task A , we want to learn the sequence of k sub-activities C_k that characterize such task, as well as the sub-activity label of all the frames of each video $v_i = \{f_n\}_{n=1}^N$, regardless of any visual differences between videos belonging to the same task.

To this end, we propose a two-stage pipeline, with the first part encoding a visual-temporal embedding and the second part encoding a temporal embedding only. The first

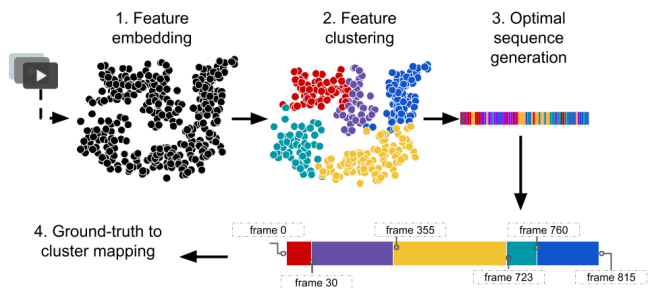


Figure 3: Unsupervised temporal segmentation pipeline. If the feature embedding has a good representation of the visual and temporal attributes of each frame, the frames that cluster together would have similar temporal locations and share visual attributes that represent a given sub-activity.

stage is trained to predict the next frame following a given input in a way that not only accurately matches the observed frame, but also allows the second stage to estimate a consistent timestamp for the output and observed frames. The resulting embedding space of the first part is then used to cluster the resulting features to form the respective classes and segment the videos accordingly. We illustrate our clustering and segmentation pipeline in Figure 3. We discuss each step of the pipeline in detail in the following sections.

3.1. Visual-temporal Embedding

To enhance the temporal nature of the video frames we model a frame prediction framework which, using as a prior the visual features of the video at time t (frame f_t) predicts the features at a future time $t + s$ (f_{t+s}). As is shown in Fig-

ure 2, our visual-temporal embedding framework consists of a linear U-Net architecture to generate an abstract representation of the frame’s features during the encoding process. The network learns to generate accurate future frame predictions by minimizing the mean squared difference between the predicted frame and the actual frame:

$$Loss_{visual} = \frac{1}{N-s} \sum_{t=1}^{N-s} (f_{t+s} - \hat{f}_{t+s})^2 \quad (1)$$

Here N is the number of video frames belonging to the task of interest, and s is the prediction time step. That is, for $s = 1$ given an input frame captured at timestamp $t = 0$ ($f_{t=0}$) the network will return a predicted frame s frames into the future ($\hat{f}_{t=1}$).

The network is composed of three down-sampling layers followed by three up-sampling layers (auto-encoder structure), the abstraction x_t generated by the last down-sampling layer is then used as the representation of the layer f_t during the sub-activity clustering process. We incorporate skip connections between the encoder and decoder to preserve fine-grained details — which might be of significance — from being discarded by the encoding process. This network structure and learning task allows us to suppress visual noise and find visual cues that are more relevant for the respective task. At the same time it ensures that the feature embedding x_t maintains enough temporally relevant information in order to reconstruct a viable future frame in the video sequence.

However, the learning objective of the model (see equation 1) is still highly oriented to the visual cues present in the video frames as we are evaluating the differences between the output \hat{f}_{t+s} of the model and the observed frame f_t . As such, to further incorporate the temporal encoding into our embedding we combine the standard U-Net architecture with a continuous temporal discriminator that is trained to estimate the timestamp of a given frame. The final architecture is then composed of (1) a frame predicting U-Net —used to extract a visual-temporal embedding from the input frames from the last down-sampling layer of the U-Net encoding section—, and (2) a timestamp predictor, trained to recognize any discrepancy between the temporal quality of the frame predicted by the U-Net \hat{f}_{t+s} and the observed frame f_t (more details on the learning task of the timestamp predictor are provided in the next section).

Using the timestamp predictor we are then able to evaluate the quality of the temporal features encoded into our embedding by evaluating the difference between the predicted timestamp of the U-Net’s output $T(\hat{f}_{t+s})$ and the predicted timestamp of the observed frame ($T(f_{t+s})$):

$$Loss_{temporal} = \frac{1}{N-s} \sum_{t=1}^{N-s} (T(f_{t+s}) - T(\hat{f}_{t+s}))^2 \quad (2)$$

To ensure that the U-Net maintains a good balance of visual and temporal cues into its embedding, its learning objective must be minimizing both the visual and temporal losses (equations 1 and 2):

$$Loss_{U-Net} = Loss_{visual} + Loss_{temporal}, \quad (3)$$

3.1.1 Temporal Embedding

The timestamp predictor is implemented as a three-layer Multilayer Perceptron (MLP) pre-trained to predict the relative timestamp of a given frame. The MLP receives as input a video frame f_t captured at a timestamp t and provides a prediction for the relative timestamp of the frame $T(f_t)$. As such, to ensure the MLP has a working knowledge on the temporal structure of the data, it must minimize the difference between the timestamp prediction $T(f_n)$ it provides for a given f_t frame, and the actual timestamp t of such frame:

$$Loss_{MLP} = \frac{1}{N} \sum_{t=1}^N (T(f_t) - t)^2 \quad (4)$$

To incorporate the timestamp predictor as a discriminator for the predictions generated by the U-Net, it must be able to identify the loss of the “temporal quality” between the frame predicted by the U-Net \hat{f}_{t+s} and the ground-truth frame f_{t+s} . Given a frame f_t we consider that the U-Net’s embedding x_t has led to the loss of temporal cues if the U-Net’s output \hat{f}_{t+s} does not have a timestamp $T(\hat{f}_{t+s})$ — timestamp estimated using the MLP— similar to the timestamp of the ground-truth frame f_{t+s} . The temporal quality (TQ) of the U-Net embedding can then be measured using the following equation:

$$TQ = \frac{1}{N-s} \sum_{t=1}^{N-s} T(\hat{f}_{t+s}) - (t+s) \quad (5)$$

We can then use the estimation of the temporal quality loss as a means for the MLP to discriminate between a real video frame f_{t+s} and a low quality estimation \hat{f}_{t+s} . As a result the timestamp predictor can learn to discriminate between the temporal differences of the U-Net’s prediction and the ground-truth. The loss of the MLP timestamp predictor is then evaluated as follows:

$$Loss_{MLP} = \left(\frac{1}{N} \sum_{t=1}^N (T(f_t) - (t))^2 \right) + (1 - TQ) \quad (6)$$

In the above formulation, $T(f_i)$ represents the output of the timestamp predictor given an input frame f_i . While this allows the U-Net to learn stronger temporal features, the reduced size of the temporal discriminator makes it prone to

over-fitting, consequently, we iterate training the timestamp predictor and the U-Net rather than having both of them learning jointly (more details on this will be discussed in the next section).

3.2. Training

We train both the U-Net and the MLP in a standalone way until they reach convergence. For the standalone training we use the visual loss indicated in equation 1 for the U-Net and the MLP loss indicated in equation 4. After this we proceed to iterate their training using the losses presented in equations 3 and 5 in conjunction with a "freeze-unfreeze" training scheme. That is, the U-Net is trained while the MLP remains frozen for x consecutive epochs, after which we would un-freeze the MLP model (and freeze the U-Net) and train for y consecutive epochs. We repeat this process until convergence of the U-Net.

3.3. Clustering and decoding

For all further processing we follow the protocol of [15, 28, 4].

Once we have the temporally enhanced embedding, we cluster the embedded features of all videos into k clusters which would later be mapped to the k sub-activities associated with the task type. We cluster the embedded features of all the videos of a given task using K-means clustering, then model each of these clusters using k Gaussian Mixtures (GMs) to obtain the per-sample average log likelihood of each frame given each of the K-GMs. As such, for every video frame n , we have a corresponding k dimensional vector with each of the frame's score for each of the clusters.

A naive approach for segmentation would be using the scores obtained by the clustering method in order to assign a sub-activity to each video frame. This however generates a non-homogeneous segmentation with few groups of continuous frames being assigned to the same sub-activity cluster. We use a modified version of the frame labeling method presented in [15], a Viterbi decoding with length model as proposed by [14] to alleviate this effect. We evaluate the probability of each frame n belonging to a cluster c_x with respect to the probabilities of the neighboring frames and seek to maximize the probability of the sequence following a fixed cluster ordering. The cluster ordering is determined by the mean time stamp of each cluster.

A fixed cluster ordering $c_1, c_2, \dots, c_i, c_j, \dots, c_k$, would constrain the possible clusters a frame f_t can be assigned to. Frame f_t could belong to either the same cluster c_i as it preceding sampled frame $f_{t-\gamma}$ -where γ is the frame sampling size (in the method introduced by [15] $\gamma = 1$) or to the next cluster c_j in the predetermined ordering .

4. Evaluation

4.1. Datasets

We evaluate our method using two datasets: Breakfast Actions dataset (BF) [12] and INRIA YouTube Instructional Videos (YTI) [2].

The Breakfast Actions dataset contains 70 hours of cooking activities of varying complexity. It contains 10 different cooking tasks (with about 170 videos per task), which can be further split into 48 sub-activities, the length of each video is highly dependent on the type of task, ranging from 30 seconds to a few minutes. The videos are recorded in different real-live environments with 52 people performing each of the ten different actions. They have a fixed view point through all 10 activities for each person, which leads to a high intra-class and low inter-class variance.

The INRIA YouTube Instructional Videos dataset contains five tasks of different instructional domains (making coffee, changing a car tire, CPR, jumping car, and potting a plant) which can be divided into 47 sub-activities. As opposed to Breakfast Actions, the videos might have been edited and include shot boundaries, as well as different and changing view points or zooming. The videos in this dataset are in average longer than the videos in Breakfast Actions, however there is a significant presence of background frames whereas the Breakfast Action actions are densely labeled without intermediate background classes.

We are using the reduced Fisher Vector features as proposed by [13] and used by [15, 28] for the evaluation of both datasets. Note that we also tried the original features provided for the YTI dataset [4], but we found the sampling of every 10th frame to be too large for a robust temporal prediction.

4.2. Evaluation Metrics

To evaluate the segmentation returned by our unsupervised approach, we need to map the segmented clusters of sub-activities to the ground-truth sub-activities related to each specific task. For this we use Hungarian matching to provide a one-to-one mapping that finds the optimal mapping that maximizes the similarity between the segmented clusters and the ground-truth sub-activities. We follow the protocol of [4, 28, 15] and compute the Hungarian matching over all videos of one activity. Note that this is different from the Hungarian matching for each single video as used by [1], which optimizes the matching for each single video and usually leads to higher accuracy, but also allows clusters to change their label from one video to another and thus gives only limited meaningful results.

We evaluate the accuracy of our method using the following metrics: the *Mean Over Frames (MoF)* to indicate the percentage of frames in the segmentation that were correctly labeled over all the frames of videos assigned to a

given task and the Jaccard Index as *Intersection Over Union (IoU)* computed for each class separately and then reported as the mean accuracy over all classes. As all datasets have a strong imbalance in terms of frame distribution, we found those two measurements to act opposing to each other, as MoF favours over-fitting on dominant classes whereas IoU favours over-fitting on underrepresented classes and therefore also consider the average of the two measures as a balance between both options.

4.3. Comparison to state-of-the-art methods

We compare the proposed model to other current approaches in the field. As is shown in Tables 1 and 2, our method performs competitively against other unsupervised and weakly supervised approaches, even outperforming one of the supervised methods. Huang *et al.* [9] classify each frame without taking into account any type of temporal information, the fact that our method manages to achieve a higher MoF value highlights the importance of incorporating temporal information into the segmentation pipeline.

It is important to note that our cluster-to ground-truth mapping and evaluation is done in a global manner, that is, we use all the predicted labels and ground-truth for all the videos of a given task to do the Hungarian matching, and then evaluate calculating the MoF and IoU using the count of all the true predictions on the whole dataset. On the other hand, approaches such as LSTM+AL [1] employ a per-video (local) cluster to ground truth mapping, which might account for the difference in the performance of the two approaches, particularly in the case of the YTI dataset, where there is a higher variance between the videos belonging to the same task.

4.4. Future frame prediction task

In order to assess the value of the future frame prediction as a good learning task that highlights the temporal nature of the data, we tested the performance of the same architecture for a step size s of 0, 1, 3, and 5 (see Figure 4 for a visual comparison of the two best performing step sizes).

When $s = 0$ the network would learn to reconstruct the same input frame from the generated abstraction, rather than generating a prediction of a future frame, with $s > 0$ the network would predict the next s_{th} frame in the video sequence following the input frame.

We can see in Table 3 the MoF and IoU obtained for the Breakfast Actions dataset. While using the U-Net to reconstruct the original input ($s = 0$) rather than to predict the next frame ($s = 1$) leads to a better performance as measured by MoF, it is important to note the decrease in the IoU of such method. In this case, the lower performance in IoU, coupled with the increase in MoF is evidence of the presence of overpopulated clusters obtained from the U-Net ($s = 0$) embedding, which leads to having a video segmen-

Supervision	Approach	MoF
Full	SVM [9]	15.8%
	TCFPN [7]	52.0%
	HTK [13]	56.3%
	GRU [25]	60.6%
Weak	Fine2Coarse [24]	33.3%
	GRU [25]	36.7%
	TCFPN+ISBA [7]	38.4%
	NN-Viterbi [26]	43%
	D3TW [5]	45.7%
	CDFL [16]	50.2%
Unsupervised	GMM [28]	34.6%
	CTE-MLP [15]	41.8%
	(LSTM+AL [1])	(42.9%*)
	Ours	42.66%

Table 1: Segmentation results on the Breakfast Action dataset compared to supervised, weakly supervised, and unsupervised state-of-the-art methods. (*denotes results with video-based Hungarian matching)

Approach	MoF	IoU	Average
GMM [28]	27.0%	—	—%
CTE-MLP [15]	39.0%	9.6%	24.3%
(LSTM+AL [1])	(60.6%*)	—	—
Ours	39.13%	9.44%	24.3%

Table 2: Segmentation results on the YTI dataset compared to unsupervised state-of-the-art methods. (*denotes results with video-based Hungarian matching). GMM [28] and LSTM+AL[1] do not provide IoU score, as such those fields were left empty in the table.

tation in which one or two activities dominate the majority of the temporal segmentation (see Figure 4). This is balanced out when moving to the prediction of future frames. Here, we see the best results for a step size of one as well as a significant decrease in both accuracy measures when the step size becomes larger.

Step size	MoF	IoU	Average
U-Net (s=0)	42.88%	9.7%	26.74%
U-Net (s=1)	41.62%	13.63%	27.62%
U-Net (s=3)	38.87%	11.61%	25.24%
U-Net (s=5)	37.41%	11.72%	24.56%

Table 3: U-Net Learning task impact on the Breakfast Actions dataset. Given an input frame captured at a time t the nU-Net was trained to estimate the frame s steps after the input frame.

Embedding	MoF	IoU	Average
U-Net	41.62%	13.63%	27.62%
MLP	40.91%	12.78%	26.85%
U-Net+MLP(U-Net)	42.66%	12.76%	27.71%
U-Net+MLP(MLP)	42.75%	10.66%	26.71%

Table 4: Analysis of the feature embedding sources on the Breakfast Actions dataset. For the full architecture, the source of the embedding can be either the U-Net or the discriminator, this is specified in parenthesis.

U-Net+MLP Loss	MoF	IoU	Average
Visual	39.66%	9.97%	24.82%
Temporal	39.35%	11.94%	25.64%
Visual+Temporal	42.66%	12.76%	27.71%

Table 5: Comparison of the effect of different losses in U-Net+MLP embedding on the Breakfast Actions dataset

4.5. Visual vs. Temporal Embedding

We also evaluate the impact of the proposed combined visual temporal embedding. To this end, we first analyze the impact of the different components of the architecture and, second, regard the impact of the proposed loss on the final system.

Table 4 shows the result of the training of the two components, the U-Net and the MLP, in a standalone way, as well as in combination. The training of the combined system results in two different embedding spaces, one from the U-Net and one from the MLP (see also Figure 2). We therefore also compare the resulting segmentation for those two different embeddings. Overall it shows that the visual embedding of the U-Net alone already leads to an increased performance of the whole system. It further shows that the best trade-off between MoF and IoU accuracy is reached with the visual embedding space of the U-Net (U-Net+MLP(U-Net))

Second, we regard the impact of the different losses on the overall system. As can be seen in Table 5, training with only the visual or temporal losses results in a decreased accuracy for MoF as well as for IoU in both cases.

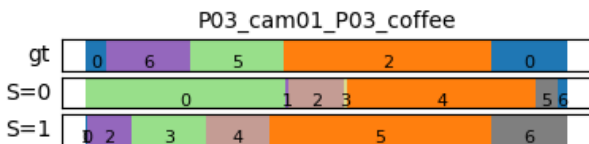


Figure 4: Segmentation illustration using different learning tasks on the U-Net architecture.

Freeze point	MoF	IoU	Average
[10, 5]	38.58%	11.44%	25.01%
[20, 5]	42.66%	12.76%	27.71%
[30, 5]	39.39%	13.00%	26.20%

Table 6: Comparison of the training intervals for the U-Net+MLP model on the Breakfast Actions dataset. A freeze point [u, m] means the U-Net was trained for u consecutive epochs -with the MLP frozen-, and then frozen for m epochs while the MLP was being trained. The freezing-unfreezing process was repeated until the network converged.

4.5.1 Freeze - unfreeze training

As the last aspect of the training pipeline, we consider the steps on the freeze-unfreeze protocol. Note that we fixed the training for the MLP to five epochs as we found that any further training leads to overfitting and adapt the training of the U-Net by using 10, 20, and 30 epochs respectively. As shown in Table 6 a training with 20 epochs leads to the highest accuracy in this case.

4.6. Clustering Analysis

We further propose in this context to use a single-GM for cluster fitting as opposed to the so far used K-GM. The motivation here is that we found that most activities tend to have a few dominant action classes, *i.e.* the two to three action classes with the most frames make up for more than 50% of the overall frames of this activity. As an example Figure 6 shows the histogram of the top seven sub-activities with respect to the overall amount of frames of the activity for two activities from the BF dataset.

The K-GM clustering method uses a localized fitting of the data where each of the K-Gaussian Mixtures is fitted using only the frames assigned to a given cluster (clusters determined using the K-means algorithm) and then provide a score on the seen and unseen frames, whereas the GM approach uses a global fitting, where a single GM observes all the frames in the task and then fits them to K distributions. It can therefore be expected that a GM-based fitting of the cluster space will be able to provide a better approximation of the underlying imbalanced cluster space than the approximation of the K-GM based clustering.

Table 7 compares the performance of the two different clustering approaches discussed in Section 3.3. We observe higher MoF scores when using the GM clustering, this however, comes at the expense of a lower IoU. The effect of this is illustrated in Figure 5 with a high imbalance in the length of the cluster segments.

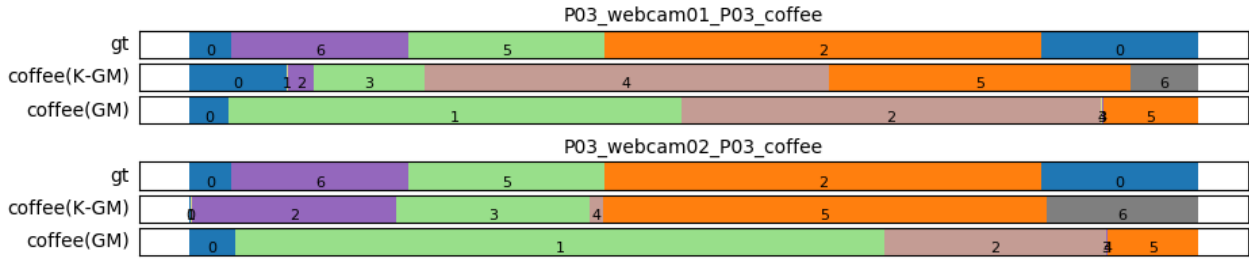


Figure 5: Segmentation illustration using different clustering methods on the U-Net embedding. Notice that the GM clustering method has a tendency of over-fitting to dominant classes.

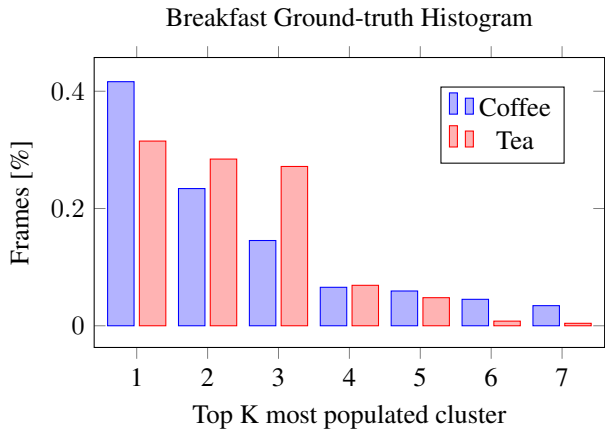


Figure 6: Sub-activity distribution for the *coffee* and *tea* tasks in Breakfast Actions. Note the imbalance in the number of frames assigned to different sub-activities

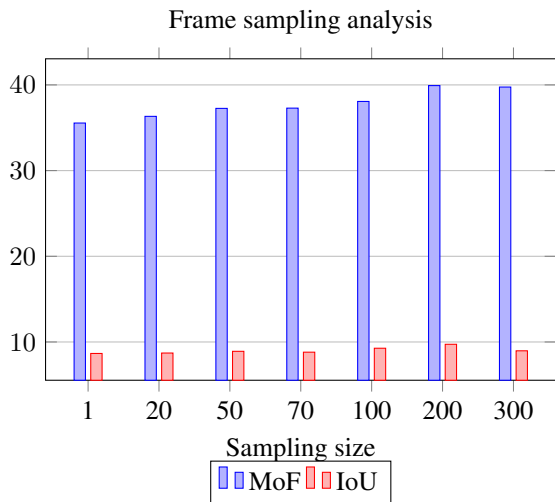


Figure 7: Analysis on the impact of frame sampling size on the YTI Dataset using the U-Net embedding.

	Clustering	MoF	IoU	Average
Breakfast	K-GM	41.62%	13.63%	27.62%
	GM	45.55%	12.31%	28.95%
YTI	K-GM	39.92%	9.73%	24.82%
	GM	47.87%	8.49%	28.15%

Table 7: U-Net Clustering method performance.

4.7. Optimal Sequence Selection

We evaluate the impact of the sampling size when calculating the labeling sequence with the highest likelihood. For this, we tested sampling sizes (γ) ranging from 1 to 300 on both datasets. While using a higher sampling size than 1 seemed to have an adverse effect on the Breakfast Actions (specially on tasks a short duration), it proved to be beneficial for the YTI videos. Figure 7 provides an analysis on the performance of the YTI Dataset when using different sampling sizes. Given that the YTI Dataset tends to have a higher percentage of irrelevant -background- frames, using a sampling size between 70 and 200 frames prevented the Viterbi code from being affected by such noisy frames.

5. Discussion

In this work we proposed an unsupervised two stage embedding pipeline that encourages the encoding of visual and temporal information of video frames for temporal segmentation tasks. We introduce a frame prediction network that makes use of a combination of predictive temporal and visual losses supported by a temporal discriminator that measures the loss of temporal quality in the embedding. We studied the impact of temporal cues through the detailed evaluation of the components of our architecture and show that training such a system in a freeze-unfreeze pipeline can lead to a significant improvement over previous approaches.

Our method was tested on two challenging datasets and achieved state-of-the-art results. The segmentations obtained with our method maintain the logical ordering of

the analyzed tasks and are able to produce coherent segments. We hope that the proposed pipeline will point to further new ideas to improve the unsupervised learning of human actions from video sequences, we suggest as future research direction addressing the incorporation of repetitive and background activities which lead to inconsistent results in their temporal location.

References

- [1] Sathyanarayanan N. Aakur and Sudeep Sarkar. A perceptual prediction framework for self supervised event segmentation. In *CVPR*, June 2019. 1, 2, 5, 6
- [2] J. Alayrac, P. Bojanowski, N. Agrawal, J. Sivic, I. Laptev, and S. Lacoste-Julien. Unsupervised learning from narrated instruction videos. In *CVPR*, pages 4575–4583, June 2016. 1, 5
- [3] Vijay Badrinarayanan, Alex Kendall, and Roberto Cipolla. Segnet: A deep convolutional encoder-decoder architecture for image segmentation. *PAMI*, 39(12):2481–2495, 2017. 3
- [4] Piotr Bojanowski, Rémi Lajugie, Francis Bach, Ivan Laptev, Jean Ponce, Cordelia Schmid, and Josef Sivic. Weakly supervised action labeling in videos under ordering constraints. In *ECCV*, pages 628–643. Springer, 2014. 1, 2, 5
- [5] Chien-Yi Chang, De-An Huang, Yanan Sui, Li Fei-Fei, and Juan Carlos Niebles. D3tw: Discriminative differentiable dynamic time warping for weakly supervised action alignment and segmentation. In *CVPR*, pages 3546–3555, 2019. 2, 6
- [6] Emily L Denton and vighnesh Birodkar. Unsupervised learning of disentangled representations from video. In I. Guyon, U. V. Luxburg, S. Bengio, H. Wallach, R. Fergus, S. Vishwanathan, and R. Garnett, editors, *NIPS*, pages 4414–4423. Curran Associates, Inc., 2017. 2, 3
- [7] Li Ding and Chenliang Xu. Weakly-supervised action segmentation with iterative soft boundary assignment. In *CVPR*, pages 6508–6516, 2018. 2, 6
- [8] Ian Goodfellow, Jean Pouget-Abadie, Mehdi Mirza, Bing Xu, David Warde-Farley, Sherjil Ozair, Aaron Courville, and Yoshua Bengio. Generative adversarial nets. In *NIPS*, pages 2672–2680, 2014. 3
- [9] De-An Huang, Li Fei-Fei, and Juan Carlos Niebles. Connectionist temporal modeling for weakly supervised action labeling. In *ECCV*, pages 137–153. Springer, 2016. 1, 2, 6
- [10] Phillip Isola, Jun-Yan Zhu, Tinghui Zhou, and Alexei A Efros. Image-to-image translation with conditional adversarial networks. In *CVPR*, pages 1125–1134, 2017. 3
- [11] Longlong Jing and Yingli Tian. Self-supervised visual feature learning with deep neural networks: A survey. *CoRR*, abs/1902.06162, 2019. 2
- [12] H. Kuehne, A. Arslan, and T. Serre. The language of actions: Recovering the syntax and semantics of goal-directed human activities. In *CVPR*, pages 780–787, June 2014. 1, 2, 5
- [13] Hilde Kuehne, Juergen Gall, and Thomas Serre. An end-to-end generative framework for video segmentation and recognition. In *WACV*, pages 1–8. IEEE, 2016. 2, 5, 6
- [14] H. Kuehne, A. Richard, and J. Gall. A hybrid rnn-hmm approach for weakly supervised temporal action segmentation. *IEEE Transactions on Pattern Analysis and Machine Intelligence*, pages 1–1, 2019. 1, 5
- [15] Anna Kukleva, Hilde Kuehne, Fadime Sener, and Juergen Gall. Unsupervised learning of action classes with continuous temporal embedding. In *CVPR*, June 2019. 1, 2, 5, 6
- [16] Jun Li, Peng Lei, and Sinisa Todorovic. Weakly supervised energy-based learning for action segmentation. In *ICCV*, pages 6243–6251, 2019. 1, 2, 6
- [17] Jonathan Long, Evan Shelhamer, and Trevor Darrell. Fully convolutional networks for semantic segmentation. In *CVPR*, pages 3431–3440, 2015. 3
- [18] William Lotter, Gabriel Kreiman, and David D. Cox. Unsupervised learning of visual structure using predictive generative networks. *ICLR*, abs/1511.06380, 2015. 3
- [19] William Lotter, Gabriel Kreiman, and David D. Cox. Deep predictive coding networks for video prediction and unsupervised learning. *ICLR*, abs/1605.08104, 2016. 3
- [20] Jonathan Malmaud, Jonathan Huang, Vivek Rathod, Nick Johnston, Andrew Rabinovich, and Kevin Murphy. What’s cookin’? interpreting cooking videos using text, speech and vision. *NAACL*, 2015. 1
- [21] Michael Mathieu, Camille Couprie, and Yann LeCun. Deep multi-scale video prediction beyond mean square error. 2015. 2, 3
- [22] Mehdi Mirza and Simon Osindero. Conditional generative adversarial nets. 2014. 3
- [23] Ishan Misra, C. Lawrence Zitnick, and Martial Hebert. Shuffle and learn: Unsupervised learning using temporal order verification. In *ECCV*, 2016. 3
- [24] Alexander Richard and Juergen Gall. Temporal action detection using a statistical language model. In *CVPR*, pages 3131–3140, 2016. 2, 6
- [25] Alexander Richard, Hilde Kuehne, and Juergen Gall. Weakly supervised action learning with rnn based fine-to-coarse modeling. In *CVPR*, pages 754–763, 2017. 2, 6
- [26] Alexander Richard, Hilde Kuehne, Ahsan Iqbal, and Juergen Gall. Neuralnetwork-viterbi: A framework for weakly supervised video learning. In *CVPR*, 2018. 6
- [27] Olaf Ronneberger, Philipp Fischer, and Thomas Brox. U-net: Convolutional networks for biomedical image segmentation. *MICCAI*, abs/1505.04597, 2015. 3
- [28] Fadime Sener and Angela Yao. Unsupervised learning and segmentation of complex activities from video. In *CVPR*, pages 8368–8376, 2018. 1, 2, 5, 6
- [29] Nitish Srivastava, Elman Mansimov, and Ruslan Salakhudinov. Unsupervised learning of video representations using lstms. In *ICML*, 2015. 3
- [30] William F. Whitney, Michael Chang, Tejas D. Kulkarni, and Joshua B. Tenenbaum. Understanding visual concepts with continuation learning. *ICLR*, abs/1602.06822, 2016. 3
- [31] Jeffrey M. Zacks and Khena M. Swallow. Event segmentation. *Current Directions in Psychological Science*, 16(2):80–84, 2007. 1
- [32] Jun-Yan Zhu, Richard Zhang, Deepak Pathak, Trevor Darrell, Alexei A Efros, Oliver Wang, and Eli Shechtman. Toward multimodal image-to-image translation. In *NIPS*, pages 465–476, 2017. 3